Article

Advances in Structural Engineering

Advances in Structural Engineering
2016, Vol. 19(1) 23–37

DOI: 10.1177/1369433215622876
ase.sagepub.com
SAGE

Discrete computational shear strength models for 5-, 6-, and 11-circular-hoop and spiral transverse reinforcement

Yu-Chen Ou[1] and Si-Huy Ngo[2]

Abstract

Based on the actual, discrete locations of interception points between the critical shear crack and transverse reinforcement, this study developed the discrete computational shear strength models for 5-, 6-, and 11-circular-hoop and spiral reinforcement. Moreover, conventional simplified calculation method was revised for use for 5-, 6-, and 11-circular-hoop and spiral reinforcement. Examination of the difference between the discrete computational shear strength models and simplified calculation shows that the error of the simplified calculation increases with increasing ratios of spacing to diameter of circular hoops or spirals. Limiting values of spacing to diameter ratios were proposed to control the error of the simplification calculation to be equal to or less than 10%. Plots of modification factors were proposed to be used with the simplification calculation when the spacing to diameter ratio is large.

Keywords

bridges, circular hoop, reinforced concrete columns, shear strength, spiral, transverse reinforcement

Introduction

It has long been recognized that columns reinforced with spiral transverse reinforcement have superior strength and ductility to those with rectilinear tie transverse reinforcement. Spiral columns showed excellent performance under extreme loading conditions such as earthquakes (e.g. Olive View Hospital in the 1971 San Fernando Earthquake (Murphy 1973)) and impact and blast loading (e.g. aircraft impact into the Pentagon building (Mlakar et al. 2005)). Due to the superior performance of spiral reinforcement, researchers and engineers have been conceiving methods to apply spiral reinforcement even in non-circular column cross sections. The first successful example is the two-spiral reinforcement scheme for oblong columns (Figure 1(a)). Results of experimental studies (Correal et al. 2004, 2007; Kawashima 2004; McLean and Buckingham 1994; Otaki and Kuroiwa 1999; Shito et al. 2002; Tanaka and Park 1993) showed that even with much less amounts of transverse reinforcement, two-spiral columns showed better strength and ductility than conventional tied columns. Recently, seven-spiral reinforcement (Figure 1(b)) was proposed for oblong columns to reduce the size of spirals to relieve difficulty in spiral fabrication when columns are large. Results of shear and flexural tests (Ou et al. 2014, 2015) showed that seven-spiral columns even with lower amounts of transverse reinforcement had superior shear and flexural capacities to conventional tied columns.

In addition to oblong columns, spiral reinforcement has been extended to square and rectangular columns. Examples include five-spiral (Figure 2(a); Yin et al. 2011, 2012) and six-spiral reinforcement (Figure 2(b); Wu et al. 2013) for square and rectangular columns, respectively. Experimental results showed five-spiral and six-spiral columns, even with less amounts of transverse reinforcement exhibited better seismic performance in terms of strength, ductility, and energy dissipation compared with conventional tied columns. Yin et al. (2011) carried out a cost evaluation of an 11-story apartment project and found that the cost of confinement reinforcement was reduced by 41% when five-spiral reinforcement was used to replace conventional tie reinforcement. Similar to the motivation of

[1]Department of Civil and Construction Engineering, National Taiwan University of Science and Technology, Taipei, Taiwan
[2]Department of Engineering and Technology, Hong Duc University, Thanhhoa, Vietnam

Corresponding author:
Yu-Chen Ou, Department of Civil and Construction Engineering, National Taiwan University of Science and Technology, Taipei, Taiwan.
Email: yuchenou@mail.ntust.edu.tw

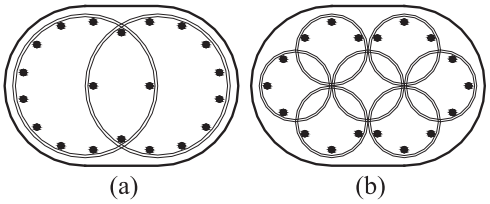

Figure 1. (a) Two-spiral reinforcement and (b) seven-spiral reinforcement.

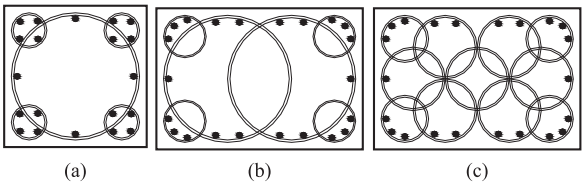

Figure 2. (a) A 5-spiral reinforcement, (b) 6-spiral reinforcement, and (c) 11-spiral reinforcement.

seven-spiral reinforcement for oblong columns, that is, reducing the size of spirals, eleven-spiral reinforcement (Ou et al. 2015) was developed by combining seven-spiral reinforcement and four smaller spirals at the corners (Figure 2(c)). Test results showed that an 11-spiral column with an amount of transverse reinforcement 75% of that of a comparable tied column exhibited better strength, ductility, and energy dissipation than the tied column.

In the shear strength design of multi-circular-hoop or multi-spiral columns, equation (1) (Caltrans, 2010 and American Association of State Highway and Transportation Officials (AASHTO), 2011) is often used to calculate shear strength provided by transverse reinforcement

$$V_s = \frac{A_v f_{yt} D}{s}, \quad \text{where } A_v = n\left(\frac{\pi}{2}\right) A_b \tag{1}$$

where V_s is the shear strength provided by transverse reinforcement, A_v the total area of transverse reinforcement within spacing s, A_b the cross-sectional area of a transverse reinforcing bar, f_{yt} the yield strength of transverse reinforcement, D the diameter of a circular hoop or spiral, s the spacing of transverse reinforcement, and n is the number of individual circular hoop sets or spirals. A hoop set refers to all the layers of hoops with their centers on the same axis parallel with the column longitudinal axis. Equation (1) is based on the studies by Ang et al. (1989) and Tanaka and Park (1993) and can be derived as follows: first, based on equilibrium and assuming transverse reinforcement yields at the ultimate condition, the shear resistance of multi-circular-hoop or multi-spiral reinforcement can be discretely computed by the following equation (Figure 3)

$$V_s = \sum_j A_{bj} f_{ytj} \sin \beta_j \sum_i \sin \alpha_i \tag{2}$$

where index j refers to the jth hoop set or spiral, index i refers to the ith intersection point within the jth hoop set or spiral, β_j is the inclination angle for the jth hoop set or spiral, and α_i is the angle for the ith intersection point (Figure 3). To simplify the discrete computation,

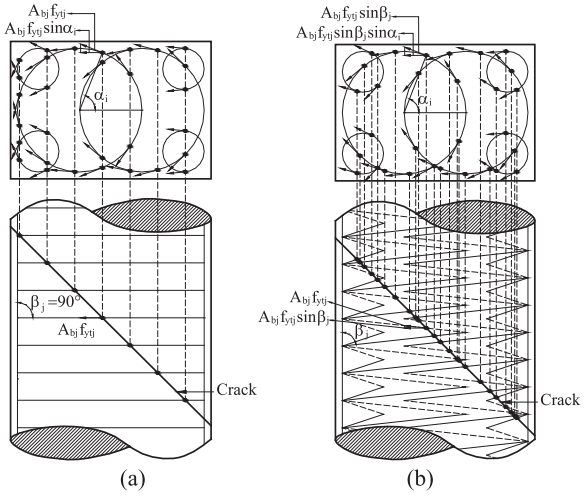

Figure 3. (a) A six-circular-hoop column and (b) a six-spiral column.

it is assumed that the vertical spacing of a circular hoop set or a spiral (s) is very small. Therefore, $\sin \beta_j \approx 1$ in the spiral case. Note that $\sin \beta_j = 1$ in the circular hoop case regardless of s. Because s is very small, the reinforcement is intersected by a shear crack at a sufficient number of points so that $\sum_i \sin \alpha_i$ from $\alpha_i = 0$ *to* π can be approximated by the summation of the average value of $\sin \alpha_i$ from $\alpha_i = 0$ *to* π, that is, $\sum_i \pi/4$. Moreover, the number of the intersection points for each circular hoop set or spiral is approximated by $2D \cot \theta/s$, where θ is the angle between the crack and longitudinal axis of the column. Hence, n circular hoop sets or spirals have $2nD \cot \theta/s$ interception points. Finally, it is assumed that the crack angle (θ) is 45° and all the hoop sets or spirals have the same bar size (A_b) and yield strength (f_{yt}). The above assumptions simplify equation (2) to equation (1) as follows

$$\begin{aligned} V_s &= \sum_j A_{bj} f_{ytj} \sin \beta_j \sum_i \sin \alpha_i \\ &= A_b f_{yt} \sum_j \sum_i \sin \alpha_i \approx A_b f_{yt}(n)\left(\frac{2D}{s}\right)\left(\frac{\pi}{4}\right) \end{aligned} \tag{3}$$

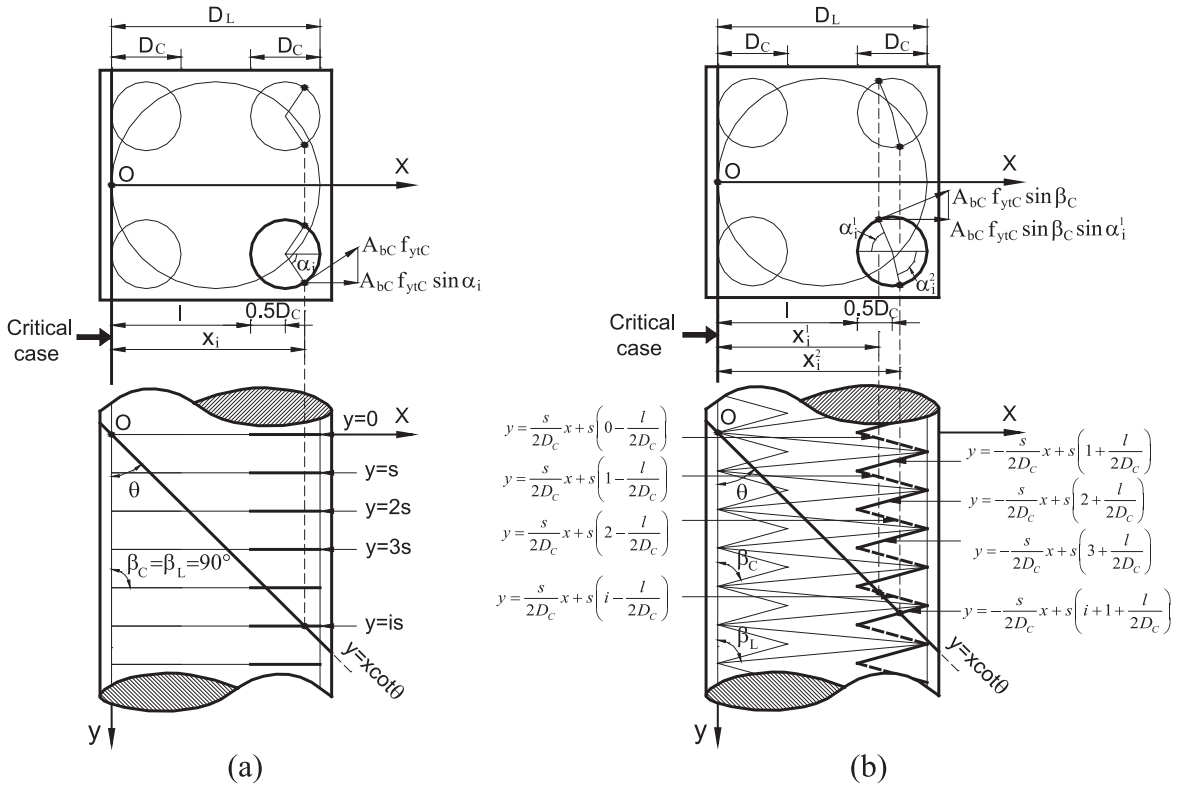

Figure 4. Discrete computational methods for shear strengths of (a) five-circular-hoop reinforcement and (b) five-spiral reinforcement.

The objective of this research is to develop the mathematical formulations of equation (2) without the small spacing-related assumptions for 5-, 6-, and 11-circular-hoop and spiral reinforcement (Figure 2) and use them to propose modifications to equation (1) for use in 5-, 6-, and 11-circular-hoop and spiral reinforcement.

Discrete computational shear strength

In this section, the mathematical formulations of equation (2), referred to as discrete computational shear strength (DCSS) models, are derived first for 5-circular-hoop and 5-spiral reinforcement and then extended to 6- and 11-circular-hoop and spiral reinforcement. In the derivation of the DCSS models, the small spacing-related assumptions used in equation (1), which include $\sin \beta_j = 1$ for spiral reinforcement, $\sum_i \sin \alpha_i = \sum_i \pi/4$, and the number of intersection points $= 2D \cot \theta/s$, are removed.

Five-circular-hoop and five-spiral reinforcement

Five-circular-hoop reinforcement. To facilitate the derivation of the DCSS model, a coordinate system is established as shown in Figure 4 to provide systematic location definition of interception points between the shear crack and transverse reinforcement. The horizontal axis (X axis) of the coordinate system is set to pass through a hoop layer. The shear crack is set to pass through the origin of the coordinate system (Figure 4(a)). Five-circular-hoop reinforcement is formed by four corner hoop sets and one central hoop set. In this subsection, a general DCSS model is derived first for a corner hoop set with the left edge a distance l from the origin of the coordinate system. Similarly, a general DCSS model is derived for a central hoop set with the left edge a distance l from the origin of the coordinate system. The DCSS model for the entire five-circular-hoop reinforcement is then formulated based on these two general DCSS models.

The right corner hoop set (with thicker lines) in Figure 4(a) is used to illustrate the derivation of the general DCSS model for a corner hoop set. As can be seen from the figure, the line function of the ith layer of the hoop set is $y = i \cdot s$. The line function of the shear crack is $y = x \cot \theta$. The interception point between the crack and the ith layer of the hoop set can be determined by solving the following simultaneous equations

$$\begin{cases} y = x \cot \theta \\ y = i \cdot s \end{cases} \Leftrightarrow x_i = is \tan \theta \tag{4}$$

The horizontal coordinate x_i of the interception point has to satisfy the following condition (from the left edge to the right edge of the hoop)

$$l \le x_i \le l + D_C \tag{5}$$

where D_C is the diameter of a corner hoop. Combining equations (4) and (5), the range for i can be obtained as follows

$$\frac{l \cot \theta}{s} \le i \le \frac{l \cot \theta}{s} + \frac{D_C}{s} \cot \theta \tag{6}$$

where $N_{D_C} = (D_C/s) \cot \theta$ and $N_l = (l/s) \cot \theta$. Note that i should be an integer. Equation (6) becomes

$$\text{int}[N_l] + 1 \le i \le \text{int}[N_l + N_{D_C}] \tag{7}$$

With trigonometry and equation (4), $\sin \alpha_i$ of equation (2) can be expressed as

$$\sin \alpha_i = \sqrt{1 - \cos^2 \alpha_i} = \sqrt{1 - \left(\frac{x_i - l - 0.5D_C}{0.5D_C}\right)^2} = \sqrt{1 - \left(\frac{0.5N_{D_C} + N_l - i}{0.5N_{D_C}}\right)^2} \tag{8}$$

Substituting equations (7) and (8) in equation (2) and noting that a hoop is intercepted at two points gives the general DCSS model for a corner hoop set

$$V_C^l = 2A_{bC}f_{ytC} \sum_i \sin \alpha_i = 2A_{bC}f_{ytC} \sum_{i = \text{int}[N_l] + 1}^{\text{int}[N_{D_C} + N_l]} \sqrt{1 - \left(\frac{0.5N_{D_C} + N_l - i}{0.5N_{D_C}}\right)^2} \tag{9}$$

where superscript l denotes that the horizontal distance from the edge of the hoop set to the origin of the coordinate system is l, subscript C denotes a corner hoop set, A_{bC} is the cross-sectional area of a corner hoop bar, and f_{ytC} is the yield strength of a corner hoop bar.

The general DCSS model for a central hoop set with the left edge a distance l from the origin of the coordinate system, V_L^l, can be derived by equations (4) to (8) with D_L substituted for D_C, where D_L is the diameter of a central hoop. Note that a larger cross-sectional diameter is often used for a central hoop because a central hoop covers a larger area than a corner hoop

$$V_L^l = 2A_{bL}f_{ytL} \sum_i \sin \alpha_i = 2A_{bL}f_{ytL} \sum_{i = \text{int}[N_l] + 1}^{\text{int}[N_{D_L} + N_l]} \sqrt{1 - \left(\frac{0.5N_{D_L} + N_l - i}{0.5N_{D_L}}\right)^2} \tag{10}$$

where subscript L denotes a central (large) hoop set; $N_{D_L} = (D_L/s) \cot \theta$, A_{bL} is the cross-sectional area of a central hoop bar, and f_{ytL} is the yield strength of a central hoop bar.

To derive the DCSS model for five-circular-hoop reinforcement, the critical shear crack needs to be set first. The critical shear crack is the one that results in the smallest shear strength and typically intercepts the edge of one or more hoop sets (as indicated by Kim and Mander 2005) because shear strength provided by interception at the edge equals to zero ($\sin \alpha_i = \sin 0° = 0$). In the case of five-circular-hoop reinforcement, the critical crack intercepts the edges of three circular hoops as shown in Figure 4(a). Based on the critical shear crack condition, five-circular-hoop reinforcement consists of two corner hoop sets with $l = 0$, two corner hoop sets with $l = D_L - D_C$, and one central hoop set with $l = 0$. For the two corner hoop sets with $l = 0$, the DCSS model for each set, V_C^0, is equation (9) with $l = 0$

$$V_C^0 = 2A_{bC}f_{ytC} \sum_i \sin \alpha_i = 2A_{bC}f_{ytC} \sum_{i = 1}^{\text{int}[N_{D_C}]} \sqrt{1 - \left(\frac{0.5N_{D_C} - i}{0.5N_{D_C}}\right)^2} \tag{11}$$

For the two corner hoop sets with $l = D_L - D_C$, the DCSS model for each set, $V_C^{D_L - D_C}$, is equation (9) with $l = D_L - D_C$

$$V_C^{D_L - D_C} = 2A_{bC}f_{ytC} \sum_i \sin \alpha_i = 2A_{bC}f_{ytC} \sum_{i = \text{int}[N_{D_L - D_C}] + 1}^{\text{int}[N_{D_C} + N_{D_L - D_C}]} \sqrt{1 - \left(\frac{0.5N_{D_C} + N_{D_L - D_C} - i}{0.5N_{D_C}}\right)^2} \tag{12}$$

where $N_{D_L - D_C} = (D_L - D_C/s) \cot \theta$. For the central hoop set with $l = 0$, the DCSS model, V_L^0, is equation (10) with $l = 0$

$$V_L^0 = 2A_{bL}f_{ytL} \sum_i \sin \alpha_i = 2A_{bL}f_{ytL} \sum_{i = 1}^{\text{int}[N_{D_L}]} \sqrt{1 - \left(\frac{0.5N_{D_L} - i}{0.5N_{D_L}}\right)^2} \tag{13}$$

The DCSS model for the entire five-circular-hoop reinforcement is

$$V_s = 2V_C^0 + 2V_C^{D_L - D_C} + V_L^0 \tag{14}$$

Five-spiral reinforcement. Similar to the derivation in the previous subsection, a coordinate system is set so that the horizontal axis (X axis) passes through the left edge

of a spiral. The shear crack is set to pass through the origin of the coordinate system (Figure 4(b)). Five-spiral reinforcement is formed by four corner spirals and one central spiral. In this subsection, the general DCSS model for a corner spiral and that for a central spiral with their edges a distance l to the origin of the coordinate system are derived first and then applied to derive the DCSS model for the entire five-spiral reinforcement. The right corner spiral in Figure 4(b) (with thicker lines) is used to illustrate the derivation of the general DCSS model for a corner spiral. To facilitate the derivation, the spiral is divided into the back side part (dash lines) and the front side part (solid lines). The line function of the dash line at the ith level is

$$y = \frac{s}{2D_C}x + s\left(i - \frac{l}{2D_C}\right) \tag{15}$$

where D_C is the diameter of a corner spiral. The line function of the solid line at the ith level is

$$y = -\frac{s}{2D_C}x + s\left(i + 1 + \frac{l}{2D_C}\right) \tag{16}$$

The line function of the crack is $y = x \cot\theta$. The x coordinate of the intersection between the crack and the ith level of the back side spiral (x_i^1) can be determined by solving the simultaneous equations of the crack line and back side spiral lines

$$x_i^1 = \frac{s\left(i - \frac{l}{2D_C}\right)}{\cot\theta - \frac{s}{2D_C}} = \frac{s(i - b_{lC})}{c_{1C}} \quad \text{from} \quad \begin{cases} y = x\cot\theta \\ y = \frac{s}{2D_C}x + s\left(i - \frac{l}{2D_C}\right) \end{cases} \tag{17}$$

where $b_{lC} = (l/2D_C)$ and $c_{1C} = \cot\theta - (s/2D_C)$. The x coordinate of the intersection point has the following range (from the left to the right edge of the spiral)

$$l \le x_i^1 \le D_C + l \tag{18}$$

Substituting equation (17) for x_i^1 in equation (18) and solving for the range of i gives

$$\frac{l\cot\theta}{s} \le i \le \frac{D_C\cot\theta}{s} + \frac{l\cot\theta}{s} - 0.5 \tag{19}$$

Note again that the i value should be integer

$$\text{int}[N_l] + 1 \le i \le \text{int}[N_{D_C} + N_l - 0.5] \tag{20}$$

With trigonometry and equation (17), $\sin\alpha_i^1$ can be expressed as

$$\sin\alpha_i^1 = \sqrt{1 - \cos^2\alpha_i^1} = \sqrt{1 - \left(\frac{l + 0.5D_C - x_i^1}{0.5D_C}\right)^2} = \sqrt{1 - \left(\frac{0.5N_{D_C} + N_l - \frac{i - b_{lC}}{c_{1C}}\cot\theta}{0.5N_{D_C}}\right)^2} \tag{21}$$

Similarly, the x coordinate of the intersection between the crack and the ith level of the front side spiral is

$$x_i^2 = \frac{s\left(i + 1 + \frac{l}{2D_C}\right)}{\cot\theta + \frac{s}{2D_C}} = \frac{s(i + 1 + b_{lC})}{c_{2C}} \quad \text{from} \quad \begin{cases} y = x\cot\theta \\ y = -\frac{s}{2D_C}x + s\left(i + 1 + \frac{l}{2D_C}\right) \end{cases} \tag{22}$$

where $c_{2C} = \cot\theta + (s/2D_C)$. The x coordinate of the intersection point has the following range

$$\frac{l\cot\theta}{s} - 1 \le i \le \frac{D_C\cot\theta}{s} + \frac{l\cot\theta}{s} - 0.5 \tag{23}$$

or

$$\text{int}[N_l] \le i \le \text{int}[N_{D_C} + N_l - 0.5] \tag{24}$$

$\sin\alpha_i^2$ can be expressed as

$$\sin\alpha_i^2 = \sqrt{1 - \left(\frac{0.5N_{D_C} + N_l - \frac{i + 1 + b_{lC}}{c_{2C}}\cot\theta}{0.5N_{D_C}}\right)^2} \tag{25}$$

Substituting equations (20), (21), (24), and (25) in equation (2) gives the general DCSS model for a corner spiral

$$V_C^l = A_{bC}f_{ytC}\sin\beta_C\sum\left(\sin\alpha_i^1 + \sin\alpha_i^2\right) = A_{bC}f_{ytC}\sin\beta_C \left[\sum_{i=\text{int}[N_l]+1}^{\text{int}[N_{D_C}+N_l-0.5]}\sqrt{1 - \left(\frac{0.5N_{D_C} + N_l - \frac{i - b_{lC}}{c_{1C}}\cot\theta}{0.5N_{D_C}}\right)^2} + \sum_{i=\text{int}[N_l]}^{\text{int}[N_{D_C}+N_l-0.5]}\sqrt{1 - \left(\frac{0.5N_{D_C} + N_l - \frac{i + 1 + b_{lC}}{c_{2C}}\cot\theta}{0.5N_{D_C}}\right)^2}\right] \tag{26}$$

where A_{bC} is the cross-sectional area of a corner spiral bar, f_{ytC} is the yield strength of a corner spiral, and $\sin\beta_C = 1/\sqrt{1 + (s/2D_C)^2}$.

Similarly, the general DCSS model for a central spiral with the left edge a distance l from the origin of the coordinate system, V_L^l, can be derived by equations

(15) to (25) with D_L substituted for D_C, where D_L is the diameter of a central spiral

$$V_L^l = A_{bL} f_{ytL} \sin\beta_L \sum \left(\sin\alpha_i^1 + \sin\alpha_i^2\right) = A_{bL} f_{ytL} \sin\beta_L \left[\sum_{i=\mathrm{int}[N_l]+1}^{\mathrm{int}\left[N_{D_L}+N_l-0.5\right]} \sqrt{1-\left(\frac{0.5N_{D_L}+N_l-\frac{i-b_{lL}}{c_{1L}}\cot\theta}{0.5N_{D_L}}\right)^2} + \sum_{i=\mathrm{int}[N_l]}^{\mathrm{int}\left[N_{D_L}+N_l-0.5\right]} \sqrt{1-\left(\frac{0.5N_{D_L}+N_l-\frac{i+1+b_{lL}}{c_{2L}}\cot\theta}{0.5N_{D_L}}\right)^2} \right] \quad (27)$$

where $\sin\beta_L = 1/\sqrt{1+(s/2D_L)^2}$, $N_{D_L} = (D_L/s)\cot\theta$, $b_{lL} = l/2D_L$, $c_{1L} = \cot\theta - (s/2D_L)$, and $c_{2L} = \cot\theta + (s/2D_L)$

Same as five-circular-hoop reinforcement, the critical shear crack in five-spiral reinforcement intercepts the edge of three spirals as shown in Figure 4(b). Based on the critical shear crack condition, five-spiral reinforcement consists of two corner spirals with $l = 0$, two corner spirals with $l = D_L - D_C$, and one central spiral with $l = 0$. For each of the corner spirals with $l = 0$, the DCSS model V_C^0 is equation (26) with $l = 0$

$$V_C^0 = A_{bC} f_{ytC} \sin\beta_C \left[\sum_{i=1}^{\mathrm{int}\left[N_{D_C}-0.5\right]} \sqrt{1-\left(\frac{0.5N_{D_C}-\frac{i}{c_{1C}}\cot\theta}{0.5N_{D_C}}\right)^2} + \sum_{i=0}^{\mathrm{int}\left[N_{D_C}-0.5\right]} \sqrt{1-\left(\frac{0.5N_{D_C}-\frac{i+1}{c_{2C}}\cot\theta}{0.5N_{D_C}}\right)^2} \right] \quad (28)$$

For each of the corner spirals with $l = D_L - D_C$, the DCSS model $V_C^{D_L-D_C}$ is equation (26) with $l = D_L - D_C$

$$V_C^{D_L-D_C} = A_{bC} f_{ytC} \sin\beta_C \left[\sum_{i=\mathrm{int}\left[N_{D_L-D_C}\right]+1}^{\mathrm{int}\left[N_{D_C}+N_{D_L-D_C}-0.5\right]} \sqrt{1-\left(\frac{0.5N_{D_C}+N_{D_L-D_C}-\frac{i-b_{(D_L-D_C)C}}{c_{1C}}\cot\theta}{0.5N_{D_C}}\right)^2} + \sum_{i=\mathrm{int}\left[N_{D_L-D_C}\right]}^{\mathrm{int}\left[N_{D_C}+N_{D_L-D_C}-0.5\right]} \sqrt{1-\left(\frac{0.5N_{D_C}+N_{D_L-D_C}-\frac{i+1+b_{(D_L-D_C)C}}{c_{2C}}\cot\theta}{0.5N_{D_C}}\right)^2} \right] \quad (29)$$

where $N_{D_L-D_C} = (D_L - D_C/s)\cot\theta$ and $b_{(D_L-D_C)C} = D_L - D_C/2D_C$

For the central spiral, the DCSS model V_L^0 is equation (27) with $l = 0$

$$V_L^0 = A_{bL} f_{ytL} \sin\beta_L \left[\sum_{i=1}^{\mathrm{int}\left[N_{D_L}-0.5\right]} \sqrt{1-\left(\frac{0.5N_{D_L}-\frac{i}{c_{1L}}\cot\theta}{0.5N_{D_L}}\right)^2} + \sum_{i=0}^{\mathrm{int}\left[N_{D_L}-0.5\right]} \sqrt{1-\left(\frac{0.5N_{D_L}-\frac{i+1}{c_{2L}}\cot\theta}{0.5N_{D_L}}\right)^2} \right] \quad (30)$$

The DCSS model for the entire five-spiral reinforcement is

$$V_s = 2V_C^0 + 2V_C^{D_L-D_C} + V_L^0 \quad (31)$$

Six-circular-hoop and six-spiral reinforcement

Similar to five-circular-hoop and five-spiral reinforcement, the critical case for shear strength of six-circular-hoop and six-spiral reinforcement is when the shear crack intercepts the edges of hoops or spirals as illustrated in Figure 5.

Under weak axis loading. The DCSS model for six-circular-hoop reinforcement under weak axis loading can be extended from that for five-circular-hoop reinforcement (equation (14)) by adding shear strength from one more central hoop (V_L^0) as defined below

$$V_s = 2V_C^0 + 2V_C^{D_L-D_C} + 2V_L^0 \quad (32)$$

where the parameters have the same definitions as equation (14). The DCSS model for six-spiral reinforcement is equation (32) with definitions of parameters same as equation (31).

Under strong axis loading. There are two potential critical cases for shear strength of six-circular-hoop or six-spiral reinforcement under strong axis loading (Figures 5(c) and 5(d)). The shear resistance of reinforcement is the smaller value obtained from the two critical cases

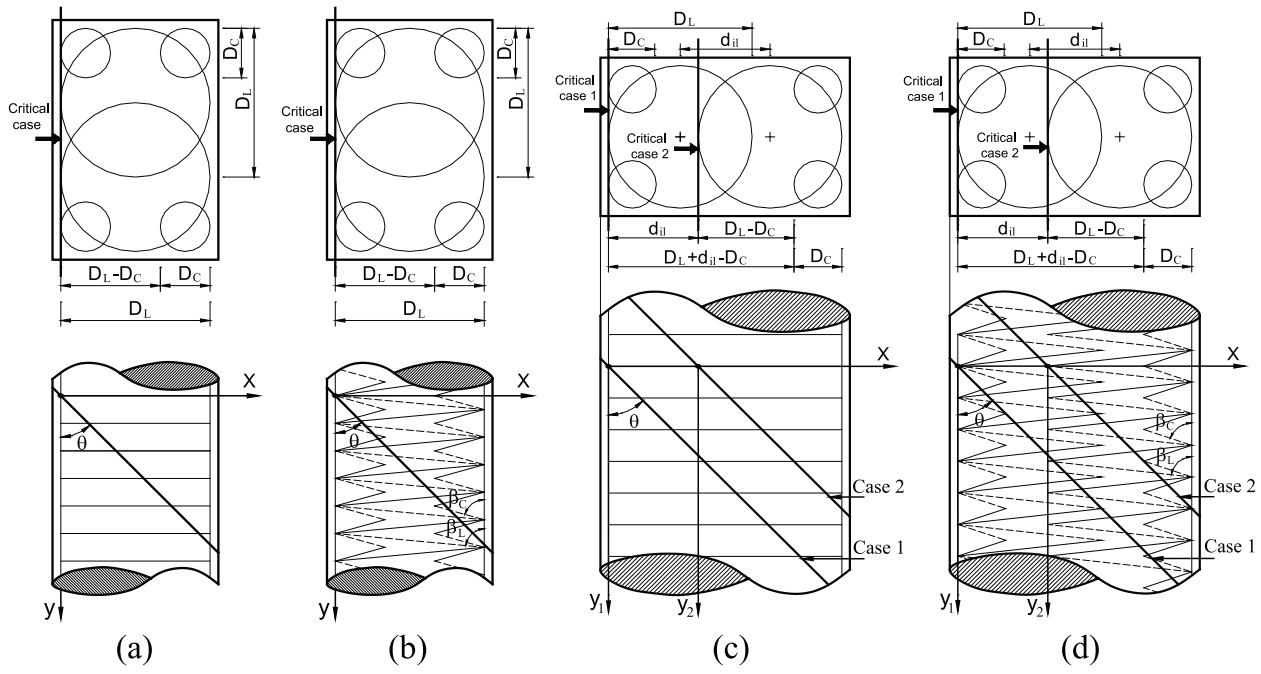

Figure 5. Discrete computational methods for shear strengths of (a) six-circular-hoop and (b) six-spiral reinforcement under weak axis loading and (c) six-circular-hoop and (d) six-spiral reinforcement under strong axis loading.

$$V_s = \min(V_1, V_2) \tag{33}$$

$$V_1 = 2V_C^0 + 2V_C^{D_L + d_{il} - D_C} + V_L^0 + V_L^{d_{il}} \tag{34}$$

$$V_2 = 2V_C^{-d_{il}} + 2V_C^{D_L - D_C} + V_L^{-d_{il}} + V_L^0 \tag{35}$$

where V_1 and V_2 are the DCSS models for critical cases 1 and 2, respectively, and d_{il} is the center-to-center spacing of the two central spirals or circular hoops. For the corner hoop sets of six-circular-hoop reinforcement, V_C^0, $V_C^{D_L + d_{il} - D_C}$, $V_C^{-d_{il}}$, and $V_C^{D_L - D_C}$ in the above equations are calculated using equation (9) with $l = 0$, $D_L + d_{il} - D_C$, $-d_{il}$, and $D_L - D_C$, respectively. For the central hoop sets, V_L^0, $V_L^{d_{il}}$, and $V_L^{-d_{il}}$ in the above equations are calculated using equation (10) with $l = 0$, d_{il}, and $-d_{il}$, respectively. Similarly, for the corner spirals of six-spiral reinforcement, V_C^0, $V_C^{D_L + d_{il} - D_C}$, $V_C^{-d_{il}}$, and $V_C^{D_L - D_C}$ are calculated using equation (26) with $l = 0$, $D_L + d_{il} - D_C$, $-d_{il}$, and $D_L - D_C$, respectively. For the central spirals, V_L^0, $V_L^{d_{il}}$, and $V_L^{-d_{il}}$ are calculated using equation (27) with $l = 0$, d_{il}, and $-d_{il}$, respectively.

Eleven-circular-hoop and 11-spiral reinforcement

Under weak and strong axis loading, there are three and four potential critical cases, respectively, for shear strength of 11-circular-hoop and 11-spiral reinforcement (Figure 6). These critical cases correspond to conditions in which the shear crack passes through the edges of hoops or spirals.

Under weak axis loading. Under weak axis loading, the shear strength of reinforcement is the smallest value obtained from the three critical cases (Figure 6(a) and (b) for circular hoop sets and spirals, respectively)

$$V_s = \min(V_1, V_2, V_3) \tag{36}$$

where V_1, V_2, and V_3 are the DCSS models for critical cases 1, 2, and 3, respectively, and are defined as follows

$$V_1 = 2V_C^0 + 2V_C^{2D_L - D_C} + 2V_L^0 + 3V_L^{0.5D_L} + 2V_L^{D_L} \tag{37}$$

$$V_2 = 2V_C^{-0.5D_L} + 2V_C^{1.5D_L - D_C} + 2V_L^{-0.5D_L} + 3V_L^0 + 2V_L^{0.5D_L} \tag{38}$$

$$V_3 = 2V_C^{-D_L} + 2V_C^{D_L - D_C} + 2V_L^{-D_L} + 3V_L^{-0.5D_L} + 2V_L^0 \tag{39}$$

where parameters on the right side of the equations are calculated by equations (9) and (10) for corner and central circular hoop sets, and equations (26) and (27) for corner and central spirals, respectively, with the superscript of the parameters substituted for l. In 11-circular-hoop and spiral reinforcement, there are 7 central and 4 corner hoop sets or spirals.

Under strong axis loading. Under strong axis loading, the shear strength of reinforcement is the smallest value obtained from the four potential critical cases

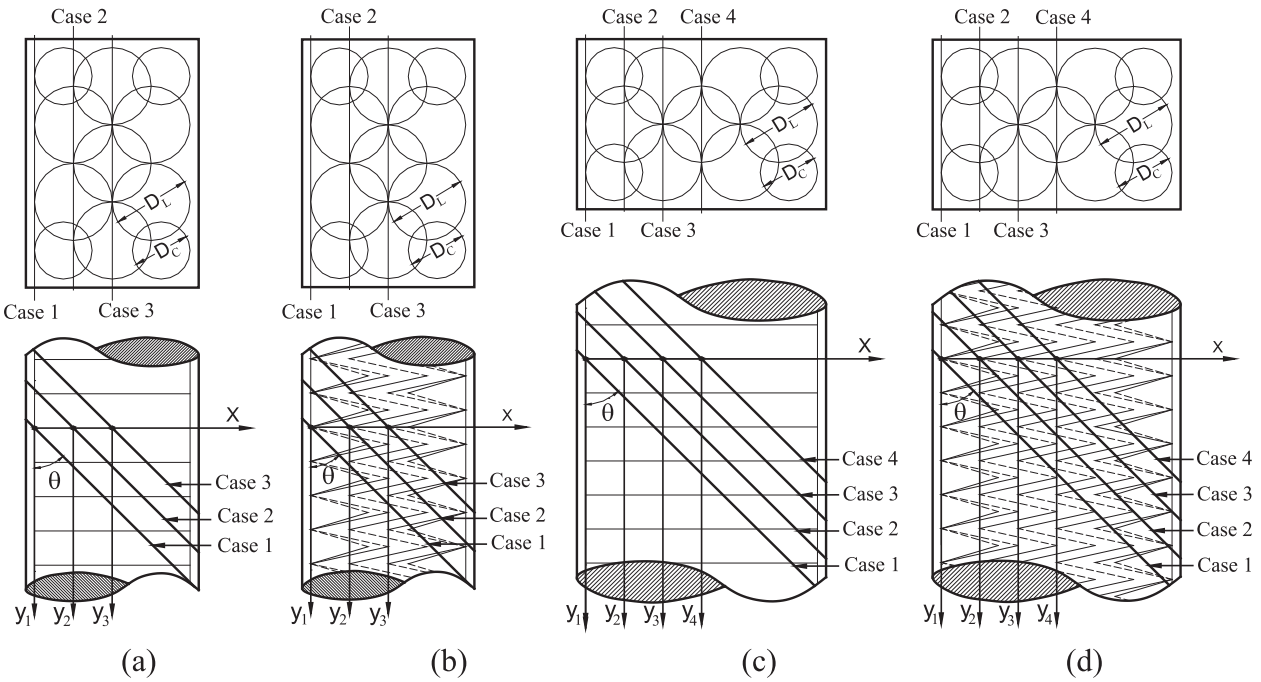

Figure 6. Discrete computational methods for shear strengths of (a) 11-circular-hoop and (b) 11-spiral reinforcement under weak axis loading and (c) 11-circular-hoop and (d) 11-spiral reinforcement under strong axis loading.

(Figure 6(c) and (d) for circular hoop sets and spirals, respectively)

$$V_s = \min(V_1, V_2, V_3, V_4) \tag{40}$$

where V_1, V_2, V_3, and V_4 are the DCSS models for cases 1, 2, 3, and 4, respectively, and are defined as follows

$$V_1 = 2V_C^0 + 2V_C^{3D_L - D_C} + V_L^0 + 2V_L^{0.5D_L} + V_L^{D_L} + 2V_L^{1.5D_L} + V_L^{2D_L} \tag{41}$$

$$V_2 = 2V_C^{-0.5D_L} + 2V_C^{2.5D_L - D_C} + V_L^{-0.5D_L} + 2V_L^0 + V_L^{0.5D_L} + 2V_L^{D_L} + V_L^{1.5D_L} \tag{42}$$

$$V_3 = 2V_C^{-D_L} + 2V_C^{2D_L - D_C} + V_L^{-D_L} + 2V_L^{-0.5D_L} + V_L^0 + 2V_L^{0.5D_L} + V_L^{D_L} \tag{43}$$

$$V_4 = 2V_C^{-1.5D_L} + 2V_C^{1.5D_L - D_C} + V_L^{-1.5D_L} + 2V_L^{-D_L} + V_L^{-0.5D_L} + 2V_L^0 + V_L^{0.5D_L} \tag{44}$$

where the parameters on the right side of the equations are defined in the same way as mentioned previously.

Simplified shear strength calculation

Equation (1) is the simplified calculation method of equation (2) and is intended for use in columns with equal-sized hoops or spirals. For 5-, 6-, and 11-circular-hoop and spiral reinforcement, the central and corner hoops or spirals have different diameters and are usually designed with bars of different sizes. They are typically designed with the same yield strength and must have the same vertical spacing. Therefore, equation (1) can be rewritten as follows for 5-, 6-, and 11-circular-hoop and spiral reinforcement

$$V_s = n_C \frac{\pi}{2} \frac{A_{bC} f_{yt} D_C}{s} + n_L \frac{\pi}{2} \frac{A_{bL} f_{yt} D_L}{s} \tag{45}$$

where n_C is the number of corner hoops or spirals and n_L is the number of central (large) hoops or spirals. It has been proposed in earlier research (Yin et al. 2011) that every hoop set or spiral in multi-circular-hoop or multi-spiral reinforcement should have the volumetric ratio ρ_s, at least equal to that required for confinement purpose. For simplicity, it is assumed that the ρ_s of the corner hoop set or spiral is equal to that of the central hoop set or spiral, that is

$$\rho_s = \frac{4A_{bL}}{D_L s} = \frac{4A_{bC}}{D_C s} \tag{46}$$

Therefore, if the diameter ratio of the central to corner hoop or spiral is denoted as $k = D_L/D_C$, then $A_{bC} = A_{bL}/k$ in order to satisfy equation (46). Equation (45) can be further rewritten as

$$V_s = \left(\frac{n_C}{k^2} + n_L\right) \frac{\pi}{2} \frac{A_{bL} f_{yt} D_L}{s} \tag{47}$$

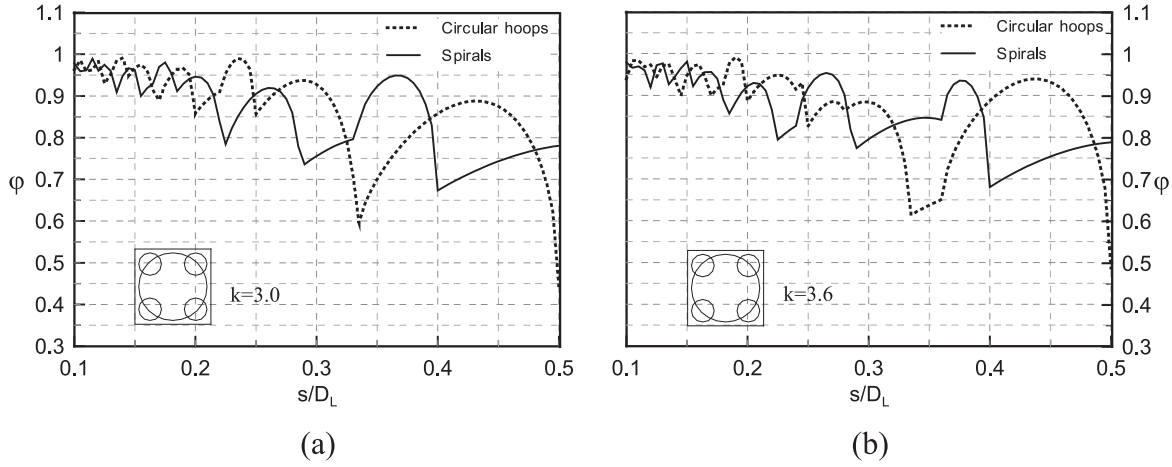

Figure 7. The φ factor for five-circular-hoop and five-spiral reinforcement: (a) $k = 3.0$ and (b) $k = 3.6$.

Relationship of DCSS models and simplified calculation

Definition of φ factor

To investigate the relationship between shear strength by the DCSS model and that by equation (47) for 5-, 6-, and 11-circular-hoop and spiral reinforcement, a φ factor is defined as follows

$$\varphi = \frac{V_s \text{ by DCSS models}}{V_s \text{ by equation(47)}} \tag{48}$$

Examination of the DCSS models and equation (47) shows that the φ factor depends on k and s/D_L. For six-circular-hoop and spiral reinforcement under strong axis loading, additionally, the φ factor depends on d_{il}. Furthermore, for 6- and 11-circular-hoop and spiral reinforcement, the φ factor also depends on the loading direction, that is, strong or weak axis loading. Note that the DCSS models are applicable to any shear crack angle (by adjusting θ). To calculate the φ factor, the angle of the critical crack, θ, used in the DCSS models is assumed to be 45°, which is the same as the crack angle adopted in the conventional simplified calculation (equation (1)).

Results of φ factor analysis

For five-circular-hoop and spiral reinforcement, the φ factor was calculated for various s/D_L and for two values of k covering the typical range of k (3.0 and 3.6; Figure 7). Similarly, for six-circular-hoop and spiral reinforcement, the φ factor was calculated for various s/D_L and $k = 3.0$ and $k = 3.6$ for both weak and strong axis loading. For strong axis loading, two values of d_{il} (R and $1.5R$) that cover the typical range of d_{il} were examined (Figure 8). For 11-circular-hoop and spiral reinforcement, the φ factor was calculated for $D_C = 0.75D_L$ ($k = 1.33$), typical in practical application (Figure 9). From Figures 7 to 9, it can be seen that the φ factor is usually lower than one, which means the simplified calculation yields shear strength higher than the DCSS model. In other words, the simplified calculation is unconservative. Moreover, the φ factor tends to decrease as the value of s/D_L increases. This means simplified calculation becomes increasingly unconservative with increasing s/D_L. This is because increasing s/D_L reduces the number of reinforcement layers intercepted by a shear crack. This tends to cause a greater difference between the actual average of $\sin \alpha_i$ and $\pi/4$, leading to a larger error when using the simplified calculation.

To control the error of the simplified calculation, the value of s/D_L should be limited if the simplified calculation is to be used without any modification. Tables 1 to 3 list the limiting values of s/D_L within which the maximum probable difference between the DCSS model and simplified calculation is $\leq 10\%$ (i.e. $\varphi \geq 0.90$) for 5-, 6-, and 11-circular-hoop and spiral reinforcement, respectively. For cases with s/D_L less than or equal to the limits in Table 1, the simplified calculation may be used without any modification. For cases with s/D_L larger than the limits, the simplified calculation can be used together with the φ factor (Figures 7 to 9) to calculate the shear strength. An example of using the simplified calculation for shear strength with the φ factor is provided in the Appendix 1.

Figure 10 compares the φ factors for 5-, 6-, and 11-circular-hoop and spiral reinforcement. In this comparison, $k = 3.0$ for five- and six-circular-hoop and spiral reinforcement and $d_{il} = R$ for six-circular-hoop and spiral reinforcement. The comparison shows that the φ factor tends to increase with increasing number of hoops or spirals for a given value of s/D_L. This is

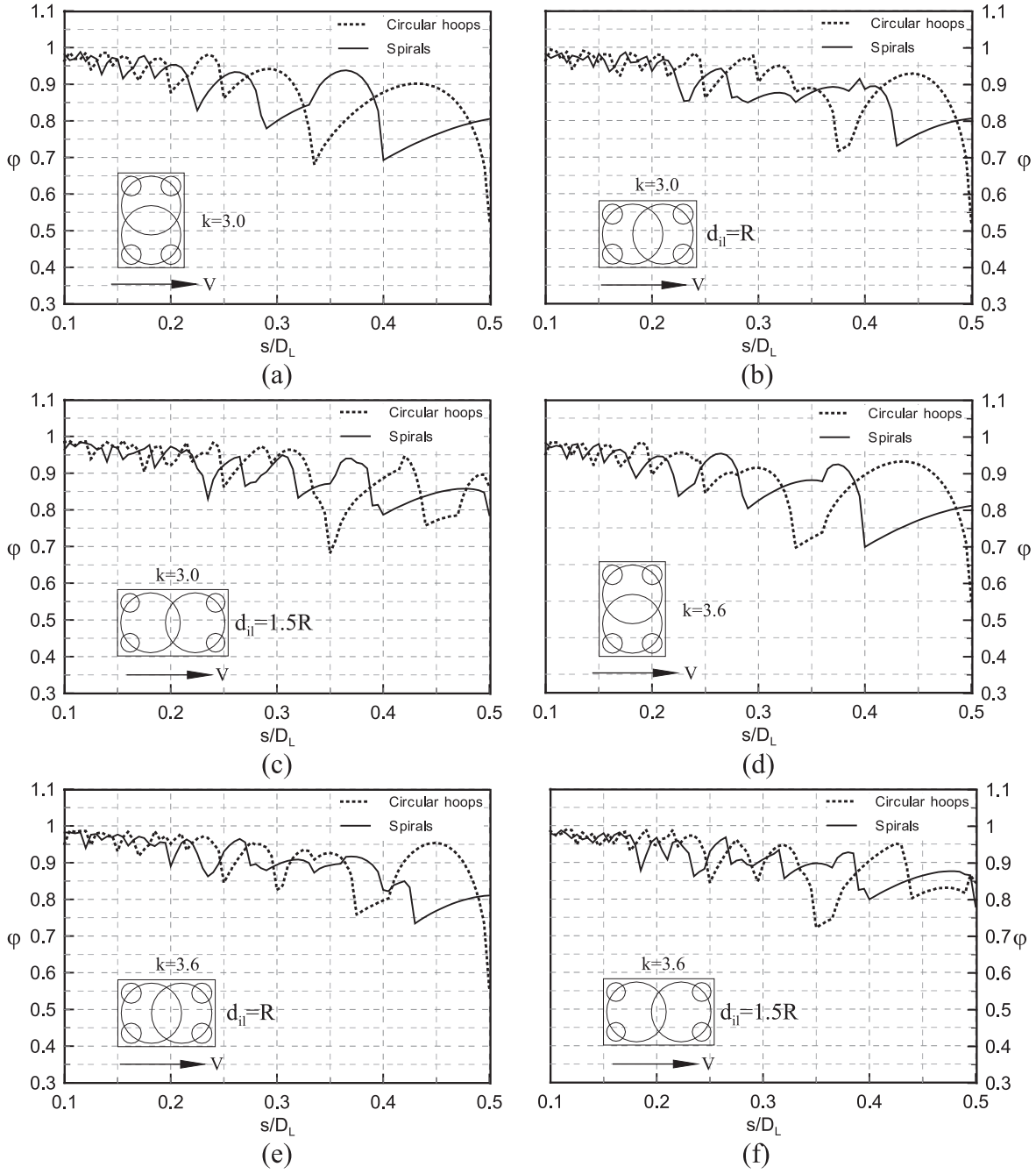

Figure 8. The φ factor for six-circular-hoop and spiral reinforcement with $k = 3$: (a) under weak axis loading; under strong axis loading with (b) $d_{il} = R$ and (c) $d_{il} = 1.5R$; with (d) $k = 3.6$ under weak axis loading; and under strong axis loading with (e) $d_{il} = R$ and (f) $d_{il} = 1.5R$.

Table 1. Limiting values of s/D_L for $\varphi \geq 0.90$ for five-circular-hoop and spiral reinforcement.

Five-circular-hoop reinforcement		Five-spiral reinforcement	
$k = 3.0$	$k = 3.6$	$k = 3.0$	$k = 3.6$
0.165	0.165	0.215	0.175

because for a given s/D_L value, increasing the number of hoops or spirals increases interception points between the shear crack and transverse reinforcement, reducing the error of using $\pi/4$ to approximate $\sin \alpha_i$ in the calculation of shear resistance. Moreover, the comparison shows that as the number of hoops or spirals increases, the φ factor curve becomes more irregular due to the increased number of critical cases.

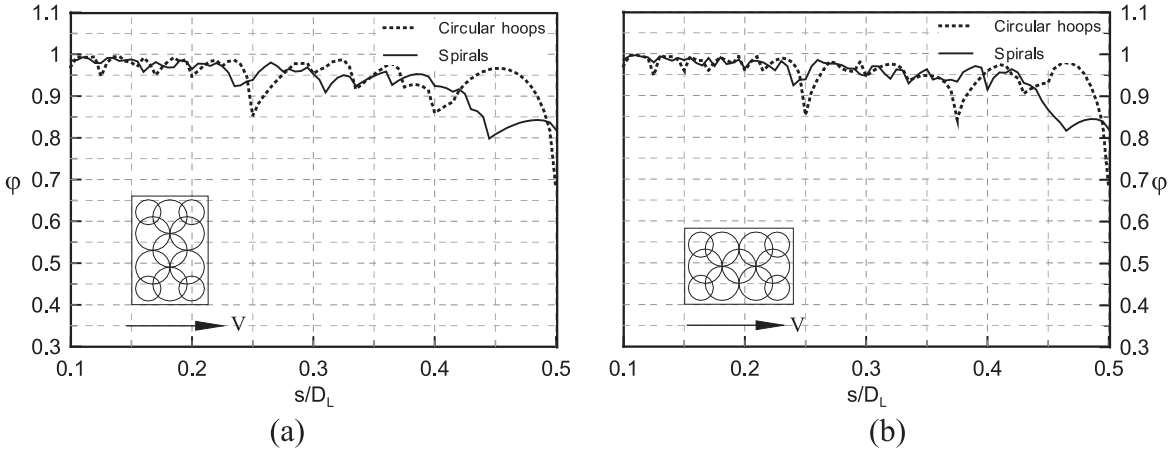

Figure 9. The φ factor for 11-circular-hoop and spiral reinforcement: (a) under weak axis loading and (b) under strong axis loading.

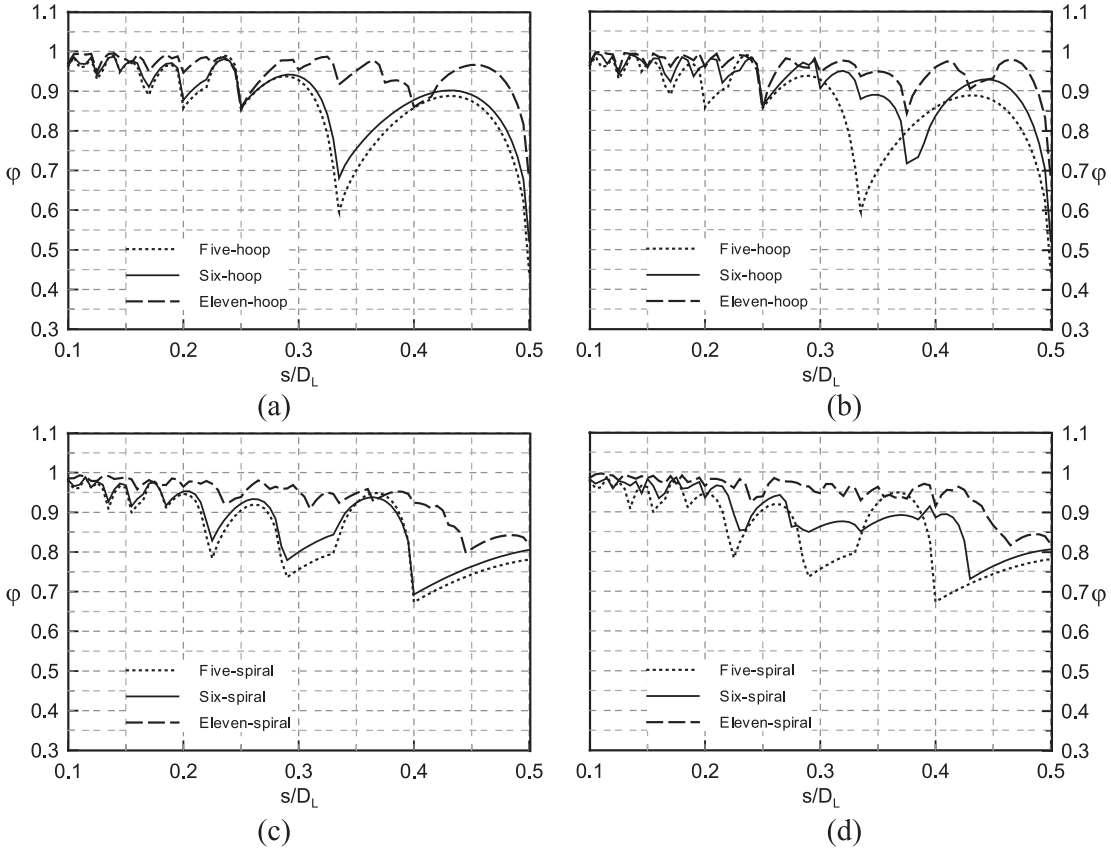

Figure 10. Comparison of the φ factor for 5-, 6-, and 11-circular-hoop reinforcement (a) under weak axis loading and (b) under strong axis loading; and for 5-, 6-, and 11-spiral reinforcement (c) under weak axis loading and (d) under strong axis loading.

Table 2. Limiting values of s/D_L for $\varphi \geq 0.90$ for six-circular-hoop and spiral reinforcement.

Case	Six-circular-hoop reinforcement		Six-spiral reinforcement	
	k = 3.0	k = 3.6	k = 3.0	k = 3.6
Weak	0.195	0.195	0.215	0.18
Strong $d_{il} = R$	0.245	0.245	0.22	0.195
Strong $d_{il} = 1.5R$	0.245	0.245	0.225	0.18

Table 3. Limiting values of s/D_L for $\varphi \geq 0.90$ for 11-circular-hoop and spiral reinforcement.

Case	Eleven-circular-hoop reinforcement	Eleven-spiral reinforcement
Weak	0.245	0.425
Strong	0.245	0.44

Conclusion

This study developed the DCSS models for 5-, 6-, and 11-circular-hoop and spiral reinforcement and examined the relationships between the DCSS models and simplified calculation method. Important conclusions are summarized as follows:

1. Based on actual, discrete locations of interception points between critical shear cracks and transverse reinforcement, the DCSS models were developed for 5-, 6-, and 11-circular-hoop and spiral transverse reinforcement. Compared with the conventional simplified shear strength calculation, which is applicable only to cases with small values of s/D_L, the DCSS models can be used for any values of s/D_L.
2. Conventional simplified shear strength calculation based on small reinforcement spacing assumption for multi-circular-hoop or multi-spiral reinforcement was revised for 5-, 6-, and 11-circular-hoop and spiral transverse reinforcement. The revised simplified calculation was divided into two parts: one for central, large hoop sets, or spirals and the other for corner hoop sets or spirals. A φ factor was proposed to be used with the simplified calculation when the value of s/D_L is large.
3. The φ factor plots show that the φ factor is usually lower than one, which means the simplified calculation is typically unconservative. Moreover, the φ factor tends to decrease, which means the simplified calculation becomes more unconservative, with increasing s/D_L due to the decreased number of interception points between the critical shear crack and transverse reinforcement. Limiting values of s/D_L were proposed for 5-, 6-, and 11-circular-hoop and spiral transverse reinforcement to control the maximum probable error of the simplified calculation to be equal to or less than 10%.

Declaration of Conflicting Interests

The author(s) declared no potential conflicts of interest with respect to the research, authorship, and/or publication of this article.

Funding

The author(s) received no financial support for the research, authorship, and/or publication of this article.

References

American Association of State Highway and Transportation Officials (AASHTO) (2011) *AASHTO Guide Specifications for LRFD Seismic Bridge Design*. Washington, DC: AASHTO.

Ang BG, Priestley MJN and Paulay T (1989) Seismic shear strength of circular reinforced concrete columns. *ACI Structural Journal* 86(1): 45–59.

Caltrans SDC (2010) *Seismic Design Criteria Version 1.6*. Sacramento, CA: California Department of Transportation.

Correal JF, Saiidi MS and Sanders DH (2004) *Seismic performance of RC bridge columns reinforced with two interlocking spirals*. Report no. CCEER-04-06, August 2004. Reno, NV: University of Nevada.

Correal JF, Saiidi MS, Sanders D, et al. (2007) Shake table studies of bridge columns with double interlocking spirals. *ACI Structural Journal* 104(4): 393–401.

Kawashima K (2004) Enhancement of flexural ductility of reinforced concrete bridge columns. In: *First international conference on urban earthquake engineering*, pp. 85–95. Tokyo, Japan: Tokyo Institute of Technology. Available at: http://www.cuee.titech.ac.jp/21coe/English/Events/Data/Papers/77kawashima.pdf

Kim JH and Mander JB (2005) Theoretical shear strength of concrete columns due to transverse steel. *ASCE Journal of Structural Engineering* 131(1): 197–199.

McLean DI and Buckingham GC (1994) *Seismic performance of bridge columns with interlocking spiral reinforcement*. Report No. WA-RD 357.1, September 1994. Washington, DC: Washington State Transportation Center.

Mlakar PF, Dusenberry DO, Harris JR, et al. (2005) Description of structural damage caused by the terrorist attack on the Pentagon. *Journal of Performance of Constructed Facilities* 19(3): 197–205.

Murphy LM (1973) *San Fernando, California, Earthquake of February 9, 1971*. Washington, DC: Department of Commerce.

Otaki T and Kuroiwa T (1999) Test of bridge columns with interlocking spiral reinforcement and conventional rectangular hoop with ties. Reports of the Technological Research institute, Tokyo Construction Co. Ltd, Tokyo, Japan, no. 25. pp. 33–38.

Ou YC, Ngo SH, Roh H, et al. (2015) Seismic performance of concrete columns with innovative seven- and eleven-spiral reinforcement. *ACI Structural Journal* 112(5): 579–592.

Ou YC, Ngo SH, Yin SY, et al. (2014) Shear behavior of oblong bridge columns with innovative seven-spiral transverse reinforcement. *ACI Structural Journal* 111(6): 1339–1349.

Shito K, Igase Y, Mizugami Y, et al. (2002) Seismic performance of bridge columns with interlocking spiral/hoop reinforcements. In: *First fib congress*, Osaka, Japan, October 2002.

Tanaka H and Park R (1993) Seismic design and behavior of reinforced concrete columns with interlocking spirals. *ACI Structural Journal* 90(2): 192–203.

Wu TL, Ou YC, Yin SYL, et al. (2013) Behavior of oblong and rectangular bridge columns with conventional tie and multi-spiral transverse reinforcement under combined axial and flexural loads. *Journal of the Chinese Institute of Engineers* 36(8): 980–993.

Yin SYL, Wang JC and Wang PH (2012) Development of multi-spiral confinements in rectangular columns for construction automation. *Journal of the Chinese Institute of Engineers* 35(3): 309–320.

Yin SYL, Wu TL, Liu TC, et al. (2011) Interlocking spiral confinement for rectangular columns. *ACI Concrete International* 33(12): 38–45.

Appendix 1

Shear strength calculation example

The cross-section of a six-spiral column is shown in Figure 11 and has the following design parameters

$$s = 85 \text{ mm}; \ \theta = 45°; \ d_{il} = R = 270 \text{ mm}$$

Corner spirals: $D_C = 180$ mm, $f_{ytC} = 490$ MPa, $A_{bC} = 28.27$ mm^2 (D6 bars)

Central spirals: $D_L = 540$ mm, $f_{ytL} = 490$ MPa, $A_{bL} = 78.54$ mm^2 (D10 bars)

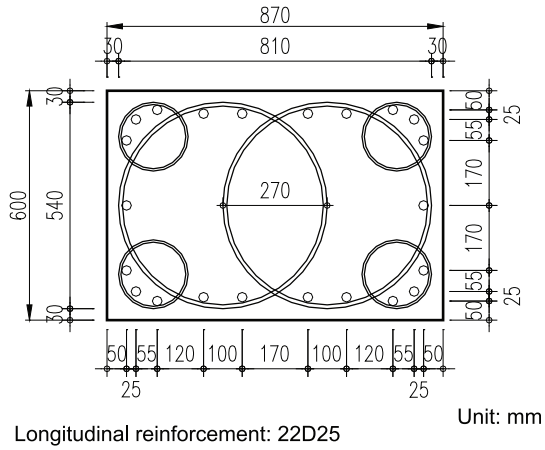

Figure 11. Cross-section design of a six-spiral column.

Shear strength by DCSS models

Shear strength provided by six-spiral transverse reinforcement under weak axis loading is calculated by equation (32)

$$V_s = 2V_C^0 + 2V_C^{D_L - D_C} + 2V_L^0 \tag{49}$$

For corner spirals

$$\sin \beta_C = \frac{1}{\sqrt{1 + \left(\frac{s}{2D_C}\right)^2}} = 0.9732$$

$$c_{1C} = \cot \theta - \frac{s}{2D_C} = 0.7639$$

$$c_{2C} = \cot \theta + \frac{s}{2D_C} = 1.2361$$

and

$$N_{D_C} = \frac{D_C}{s} \cot \theta = 2.12$$

For $l = 0$

$$b_{lC} = \frac{l}{2D_C} = 0$$

and

$$N_l = \frac{l}{s} \cot \theta = 0$$

$$V_C^0 = A_{bC} f_{ytC} \sin \beta_C \left[\sum_{i=1}^{\text{int}[N_{D_C} - 0.5]} \sqrt{1 - \left(\frac{0.5N_{D_C} - \frac{i}{c_{1C}} \cot \theta}{0.5N_{D_C}} \right)^2} + \sum_{i=0}^{\text{int}[N_{D_C} - 0.5]} \sqrt{1 - \left(\frac{0.5N_{D_C} - \frac{i+1}{c_{2C}} \cot \theta}{0.5N_{D_C}} \right)^2} \right] = 37,655 \text{ N}$$

For $l = D_L - D_C = 360$ mm

$$b_{lC} = \frac{l}{2D_C} = 1$$

and

$$N_l = \frac{l}{s} \cot \theta = 4.23$$

$$V_C^{l=360} = A_{bC} f_{ytC} \sin \beta_C \left[\sum_{i=\text{int}[N_l]+1}^{\text{int}[N_{D_C} + N_l - 0.5]} \sqrt{1 - \left(\frac{0.5N_{D_C} + N_l - \frac{i - b_{lC}}{c_{1C}} \cot \theta}{0.5N_{D_C}} \right)^2} + \sum_{i=\text{int}[N_l]}^{\text{int}[N_{D_C} + N_l - 0.5]} \sqrt{1 - \left(\frac{0.5N_{D_C} + N_l - \frac{i+1+b_{lC}}{c_{2C}} \cot \theta}{0.5N_{D_C}} \right)^2} \right]$$

$$= 38,366 \text{ N}$$

For central spirals

$$\sin\beta_L = \frac{1}{\sqrt{1+\left(\frac{s}{2D_L}\right)^2}} = 0.9969$$

$$c_{1L} = \cot\theta - \frac{s}{2D_L} = 0.9213$$

$$c_{2L} = \cot\theta + \frac{s}{2D_L} = 1.0787$$

and

$$N_{D_L} = \frac{D_L}{s}\cot\theta = 6.35$$

For $l = 0$

$$b_{lL} = \frac{l}{2D_L} = 0 \text{ and } N_l = \frac{l}{s}\cot\theta = 0$$

$$V_L^0 = A_{bL}f_{ytL}\sin\beta_L\left[\sum_{i=1}^{\text{int}\left[N_{D_L}-0.5\right]}\sqrt{1-\left(\frac{0.5N_{D_L}-\frac{i}{c_{1L}}\cot\theta}{0.5N_{D_L}}\right)^2} + \sum_{i=0}^{\text{int}\left[N_{D_L}-0.5\right]}\sqrt{1-\left(\frac{0.5N_{D_L}-\frac{i+1}{c_{2L}}\cot\theta}{0.5N_{D_L}}\right)^2}\right] = 363,666\,\text{N}$$

Shear strength under weak axis loading is

$$V_s = 2V_C^0 + 2V_C^{D_L-D_C} + 2V_L^0 = 879\,\text{kN}$$

Shear strength provided by six-spiral transverse reinforcement under strong axis loading is calculated by equation (33)

$$V_s = \min(V_1, V_2) \tag{50}$$

where

$$V_1 = 2V_C^0 + 2V_C^{D_L+d_{il}-D_C} + V_L^0 + V_L^{d_{il}} \tag{51}$$

$$V_2 = 2V_C^{-d_{il}} + 2V_C^{D_L-D_C} + V_L^{-d_{il}} + V_L^0 \tag{52}$$

$$V_C^{-d_{il}=-270} = 50,689\,\text{N}$$

$$V_C^{D_L+d_{il}-D_C=630} = 43,847\text{N}$$

$$V_L^{d_{il}=270} = 373,914\text{N}$$

$$V_L^{-d_{il}=-270} = 386,786\,\text{N}$$

$$V_1 = 2V_C^0 + 2V_C^{D_L+d_{il}-D_C} + V_L^0 + V_L^{d_{il}} = 901\,\text{kN}$$

$$V_2 = 2V_C^{-d_{il}} + 2V_C^{D_L-D_C} + V_L^{-d_{il}} + V_L^0 = 929\,\text{kN}$$

$$V_s = \min(V_1, V_2) = 901\,\text{kN}$$

Shear strength by simplified calculation method

From equation (45)

$$V_s = \varphi\left(n_C\frac{\pi}{2}\frac{A_{bC}f_{ytC}D_C}{s} + n_L\frac{\pi}{2}\frac{A_{bL}f_{ytL}D_L}{s}\right) \tag{53}$$

where $n_C = 4$ (number of corner spirals) and $n_L = 2$ (number of central spirals)

$$\frac{s}{D_L} = 0.16$$

Under weak axis loading with $k = D_L/D_C = 540/180 = 3.0$: $\varphi = 0.92$ (Figure 8(a))

$$V_s = \varphi\left(n_C\frac{\pi}{2}\frac{A_{bC}f_{ytC}D_C}{s} + n_L\frac{\pi}{2}\frac{A_{bL}f_{ytL}D_L}{s}\right) = 0.92\times\left(4\times\frac{\pi}{2}\times\frac{28.27\times490\times180}{85} + 2\times\frac{\pi}{2}\frac{78.54\times490\times540}{85}\right) = 876,210\,\text{N}\approx876\,\text{kN}$$

Under strong axis loading with $k = 3.0$ and $d_{il} = R$: $\varphi = 0.93$ (Figure 8(b))

$$V_s = \varphi\left(n_C\frac{\pi}{2}\frac{A_{bC}f_{ytC}D_C}{s} + n_L\frac{\pi}{2}\frac{A_{bL}f_{ytL}D_L}{s}\right) = 0.93\times\left(4\times\frac{\pi}{2}\times\frac{28.27\times490\times180}{85} + 2\times\frac{\pi}{2}\frac{78.54\times490\times540}{85}\right) = 885,734\,\text{N}\approx886\,\text{kN}$$

If φ is not applied for equation (45), under both weak and strong axis loading

$$V_s = n_C\frac{\pi}{2}\frac{A_{bC}f_{ytC}D_C}{s} + n_L\frac{\pi}{2}\frac{A_{bL}f_{ytL}D_L}{s} = 4\times\frac{\pi}{2}\times\frac{28.27\times490\times180}{85} + 2\times\frac{\pi}{2}\frac{78.54\times490\times540}{85} = 952,402\,\text{N}\approx952\,\text{kN}$$

Table 4 summarizes calculation results. Note that $s/D_L = 0.16$, which is less than the limiting values of

Table 4. Comparison of calculation results.

Loading direction	Shear strength (kN)		
	DCSS model	Simplified model w/o φ	Simplified model with φ
Weak axis	879	952	876
Strong axis	901	952	886

DCSS: discrete computational shear strength.

s/D_L for weak and strong axis loading in Table 2 (0.215 and 0.22, respectively). Therefore, the differences between the DCSS models and simplified calculation without the φ factor are expected to be less than 10%. The actual differences are 8.3% and 5.7% for weak and strong axis loading, respectively. With the use of the φ factor, the difference is reduced to be less than 2%. Another observation from Table 4 is that without the φ factor, the simplified calculation is not able to reflect the difference in shear strength between two loading directions.